HHS Public Access

Author manuscript

Nat Cell Biol. Author manuscript; available in PMC 2015 June 01.

Published in final edited form as:

Nat Cell Biol. 2014 December ; 16(12): 1146–1156. doi:10.1038/ncb3070.

SOX17 links gut endoderm morphogenesis with germ layer segregation

Manuel Viotti[1,2,*], **Sonja Nowotschin**[1], and **Anna-Katerina Hadjantonakis**[1,#]

[1]Developmental Biology Program, Sloan Kettering Institute, 1275 York Avenue, New York, NY 10065, USA

[2]Biochemistry, Cell and Molecular Biology Program, Weill Graduate School of Medical Sciences of Cornell University, New York, NY 10065, USA

Abstract

Gastrulation leads to three germ layers, ectoderm, mesoderm and endoderm that are separated by two basement membranes. In the mouse embryo, the emergent gut endoderm results from the widespread intercalation of cells of two distinct origins: pluripotent epiblast-derived definitive endoderm (DE) and extra-embryonic visceral endoderm (VE). Here we image the trajectory of prospective DE cells prior to intercalating into the VE epithelium. We show that the transcription factor SOX17, which is activated in prospective DE cells prior to intercalation, is necessary for gut endoderm morphogenesis and the assembly of the basement membrane that separates gut endoderm from mesoderm. Our results mechanistically link gut endoderm morphogenesis and germ layer segregation, two central and conserved features of gastrulation.

Keywords

mouse embryo; gastrulation; gut endoderm; mesoderm; epiblast; intercalation; egression; SOX17; FOXA2; ECM; basement membrane; apico-basal polarity; Integrin; Fibronectin

INTRODUCTION

Gastrulation is a choreographed sequence of cell fate specification, proliferation and movement that results in the generation of the three embryonic germ layers; ectoderm, mesoderm and definitive endoderm. During gastrulation, pluripotent epiblast cells ingress through the transient primitive streak and undergo an epithelial-to-mesenchymal transition (EMT). Ingressing cells emerge as mesoderm and definitive endoderm (DE)[1]. These cells collectively migrate in the space between the adjacent epithelia of the epiblast and visceral endoderm (VE). As a paradigm for tissue growth and remodeling, gastrulation in amniotes

[#]Author for correspondence: hadj@mskcc.org; 1-212-639-3159 (phone); 1-646-422-2355 (FAX).
[*]Present address: Genentech, 1 DNA Way, South San Francisco, CA 94080, USA

AUTHOR CONTRIBUTIONS

AKH conceived the project. MV, SN and AKH designed the experiments and interpreted results. MV and SN carried out the experiments. MV and AKH wrote the manuscript with input from SN.

transforms the embryo comprising the epiblast and adjacent VE, into a three-layered configuration comprising epiblast/ectoderm, mesoderm and gut endoderm[2, 3].

The gut endoderm arises as an epithelium on the embryo's surface. It gives rise to the multipotent progenitors of the respiratory and digestive tracts, and their associated organs[4]. Our previous work revealed that in the mouse emergent gut endoderm comprises cells of two distinct origins, DE and VE, arising from the widespread intercalation of these two cell populations[5–7]. The cell behaviors associated with this morphogenetic event are not well understood.

Here we have investigated the molecular programs and behaviors of DE and VE cells during mouse gut endoderm morphogenesis. Using 3D time-lapse imaging we tracked presumptive DE progenitors from the primitive streak into the mesoderm layer and onto the embryo surface where they intermingled with embryonic VE (emVE) cells[8]. By analyzing different mutants exhibiting gastrulation and endoderm defects, we demonstrate that DE cells must polarize and modulate extracellular matrix (ECM) components, undergoing a mesenchymal-to-epithelial transition (MET)to insert into the emVE epithelium. The Sry-related HMG-box containing transcription factor SOX17 is a key orchestrator of this egression. To facilitate the egression of prospective DE cells, the emVE epithelium must coordinately and transiently modulate their apico-basal polarity, cell-cell junctions and basement membrane (BM) composition. Altogether, our observations reveal an association between gut endoderm morphogenesis and BM assembly, two cardinal features of gastrulation, and implicate SOX17 in a genetic program coordinating these events.

RESULTS

Live imaging and tracking of DE progenitors from the primitive streak to the embryo's surface

To follow the trajectories and behavior of DE progenitors from their origin within the primitive streak to their destination in the gut endoderm, we combined live imaging with transient and transgenic fluorescent cell labeling. We electroporated a plasmid driving widespread expression of a red fluorescent protein (RFP) into the posterior epiblast of *Afp::GFP* transgenic embryos (Fig. 1a). The *Afp::GFP* reporter permitted visualization of VE cells[6, 9]. Embryos were cultured after electroporation and those exhibiting normal morphology with detectable RFP expression at the primitive streak, were 3D time-lapse imaged (Fig. 1a–e and Supplementary Video 1). Over time, RFP-positive cells were identified in an anterior-ward stream (Fig. 1c–e and Supplementary Video 2). Close inspection of RFP-positive cells suggested they underwent an EMT. Surface renderings revealed an initially uniform GFP-positive layer. Over time, GFP-negative regions appeared, with a subset being RFP-positive (Fig. 1b′–e′ and Supplementary Video 3). Tracking identified trajectories adopted by prospective DE cells during gastrulation: DE progenitors initially reside in the posterior epiblast, ingress through the primitive streak, and emerge onto the embryo surface by multi-focally inserting into the emVE (Supplementary Videos 1–5).

Cells egress into the visceral endoderm from within the wings of mesoderm

We next imaged sequentially staged embryos expressing the pan-VE *Afp::GFP* reporter before, during and after emVE dispersal. At the pre-streak (PS) stage (embryonic day (E) 6.25), a uniform GFP distribution was observed on the embryo surface, indicating that emVE dispersal had not commenced (Fig. 1f). Transverse sections through the embryonic region identified two epithelia: a columnar epithelium comprised of the inner epiblast and a squamous epithelium comprised of the outer emVE (Fig. 1f′). By the late streak (LS) stage (E7.0), surface renderings revealed a few GFP-negative areas present within the GFP-positive emVE layer, presumably representing the first DE cell cohort that egressed onto the embryo's surface (Fig. 1g). Transverse sections identified mesoderm positioned between the epiblast and outer emVE (Fig. 1g′, leading-edge of mesoderm, orange asterisk). A subset of GFP-negative cells, which aligned with the mesoderm located adjacent to the emVE, were indenting into the overlying GFP-positive emVE layer (Fig. 1g′, inset, white arrowheads) likely representing DE progenitors in the process of egression.

Notably, egressing cells, defined either as GFP-negative regions on the embryo's surface in 3D renderings or regions of indentations in the GFP-positive layer in transverse sections, were not observed anterior to the mesoderm's leading-edge, suggesting that DE progenitors are incorporated within or travel alongside the mesoderm. By the no bud (OB) stage (E7.25), embryos exhibited extensive emVE dispersal (Fig. 1h). Sections revealed that some GFP-negative cells already embedded in the surface epithelium (red arrowheads), while others were in the process of egressing, still enveloped by GFP-positive areas (Fig. 1h′, inset, white arrowheads). By the late bud (LB)/early head-fold (EHF) stage (E7.5), when emVE dispersal was complete, GFP-positive regions comprised isolated cells (Fig. 1i). Transverse sections confirmed that, at this time, the mesoderm had completed its migration, and the embryo's surface was composed of both GFP-positive emVE-descendants and GFP-negative epiblast-derived DE cells (Fig. 1i′).

Gastrulation mutants do not undergo visceral endoderm dispersal

To analyze the genetic control of egression, we assessed emVE dispersal in embryos exhibiting defects in gastrulation. Mutants in FGF signaling components, including FGF8 or FGFR1, specified mesoderm, but cells failed to migrate away from the primitive streak[10–12]. Prior to gastrulation, *Fgf8* or *Fgfr1* mutant embryos were indistinguishable from wild-type littermates. However, by the OB stage (E7.25,) when emVE dispersal was underway in wild-type embryos, *Fgf8* or *Fgfr1* mutants exhibited a complete failure in emVE dispersal. Sections confirmed a failure in mesoderm migration (Fig. 1j, 1j′ and Supplementary Fig. 1a, a′ and 1b,1b′). The T-box transcription factor EOMESODERMIN (EOMES) plays a critical role in both anterior visceral and definitive endoderm specification[13, 14]. Its ablation in the epiblast (*Eomes*$^{epi\Delta}$) leads to cell accumulations at the primitive streak and defects in mesodermal migration and endoderm specification[15]. Like FGF signaling mutants, *Eomes*$^{epi\Delta}$ embryos exhibited a failure of emVE dispersal (Supplementary Fig. 1c, c′), confirming that proper migration of mesoderm cells away from the primitive streak is necessary for VE dispersal and DE formation.

SOX17 and FOXA2 mark definitive endoderm cells prior to and during egression

We next investigated whether DE progenitors were molecularly distinct from neighbouring mesoderm cells prior to their egression onto the embryo's surface. Analysis of SOX17, an evolutionarily conserved factor critical for endoderm specification[16, 17], revealed it to be expressed by DE cells prior to, during and after egression. Before emVE dispersal had started, SOX17 was detected at low levels throughout the emVE (Supplementary Fig. 2a–b′, g). During early stages of emVE dispersal (E7.0), high SOX17 levels were detected in a subset of cells present within the mesoderm layer, making contact with the emVE (Fig. 2a–c and Supplementary Fig. 2g), suggesting these could be presumptive DE cells in the process of egression. By completion of emVE dispersal (Fig. 2e, finsets), SOX17 was detected at equivalently high levels in both DE and emVE-derived cells (Fig. 2d–f and Supplementary Fig. 2g).

The distribution of FOXA2, another conserved factor important in the specification and formation of endoderm[18], was comparable to SOX17 at these stages and in this region of the embryo (Supplementary Fig. 2h–n). SOX17 and FOXA2 colocalization exhibited a strong correlation (Supplementary Fig. 2o–v). In contrast to SOX17, FOXA2 was, however, expressed at lower levels in some posterior epiblast cells prior to their ingression through the primitive streak (Supplementary Fig. 2y), and was robustly expressed later in midline structures[7] (Supplementary Fig. 2w, x).

SOX17 is required for definitive endoderm cell egression

We investigated gut endoderm morphogenesis in *Sox17* mutants as embryos lacking *Sox17* are deficient in the midgut and hindgut DE, with endoderm cells having been reported as exhibiting a VE-like morphology[16]. At the LS stage (E7.0), when DE cells have normally started to egress, *Sox17* mutant embryos exhibited a uniform layer of GFP-positive cells on their surface, suggesting DE progenitors had not egressed (Fig. 2g). By the LB/EHF stage (E7.5), when emVE dispersal is normally complete, the emVE appeared as a uniform, GFP-positive epithelial sheet in *Sox17* mutants (Fig. 2h), except the prospective foregut region (Fig. 2h, white arrowhead). Sections through *Sox17* mutants confirmed that gastrulation had occurred, as the embryo comprised three tissue layers, with the surface layer exclusively comprised emVE (Fig. 2i, j).

Definitive endoderm cell egression occurs in the absence of FOXA2

Gut endoderm morphogenesis was also analyzed in *Foxa2* mutants, which exhibited an overall growth retardation with failure to form midline structures (Fig. 3a–d, see orange arrowhead). In contrast to *Sox17* mutants, dispersal of the emVE appeared to occur in the absence of FOXA2 (Fig. 3b, see white arrowhead). SOX17 was expressed in *Foxa2* mutants (Fig. 3c–d). FOXA2 expression was also unperturbed in *Sox17* mutants, with mesodermal cells adjacent to the emVE exhibiting high levels of FOXA2, as in wild-type embryos (Supplementary Fig. 2s–v′).

Cells failing to execute a program of definitive endoderm differentiation are retained within the mesoderm layer

To investigate the fate of DE progenitors in *Sox17* mutants, we used a *Sox17*^{GFP} line[19]. Perdurance of GFP served as a short-term cell lineage tracer. In LB/EHF stage *Sox17*$^{GFP/+}$ embryos, GFP was detected in a belt of cells on the embryo surface, DE and emVE-derived cells comprising the gut endoderm (Fig. 4a–d). By contrast, in *Sox17*$^{GFP/GFP}$ embryos, an additional population of GFP-positive cells was present within the mesoderm layer (Fig. 4a′–d′). The SOX17-GFP-positive cells embedded within the mesoderm likely arose because of a failure in egression and in the DE program. These “trapped” non-egressed cells did not express FOXA2, suggesting they did not acquire a DE identity (Fig. 4c′). However, FOXA2 was expressed at earlier stages in *Sox17* mutants (see Supplementary Fig. 2u′), suggesting that when DE cells failed to egress, they did not maintain expression of endoderm markers.

We noted that trapped SOX17-GFP-positive cells exhibited low levels of E-CADHERIN, which normally marks epithelial cells, suggesting cell polarization was initiated (Fig. 4e–h′, orange arrowheads). The presence of N-CADHERIN, which is exclusively localized in mesodermal cells, indicated that the trapped cells had acquired the mesenchymal character of their mesoderm neighbours (Fig. 4i–l′, orange arrowheads, and Supplementary Fig. 3a–c).

Gastrulation involves a transition from one to two basement membranes

Epithelia commonly reside on extracellular matrix (ECM) proteins that collectively form a basement membrane (BM). BMs provide rigidity and separation between adjacent tissue layers. The acquisition of three germ layers at gastrulation is accompanied by a transition from a single BM present at the epiblast-emVE interface, to two BMs, one positioned at the epiblast-mesoderm interface, and another at the mesoderm-endoderm interface. If DE cells were traversing layers, they would need to remodel the BM at the mesoderm-endoderm interface. Hence, an absence of ECM proteins could be expected in their vicinity. We analyzed ECM protein distribution at the time of DE cell egression. At the mid-emVE dispersal stage FIBRONECTIN-1 (FN-1), a critical BM factor, was localized in two belts at the epiblast-mesoderm and the mesoderm-endoderm interfaces (Fig. 5g–i′). GFP-negative DE cells and GFP-positive emVE cells were positioned on the same side of the BM. Since we were unable to reconcile these observations with a model of BM breakdown by egressing DE cells, we determined ECM factor distribution during successive stages of DE cell egression and emVE dispersal.

At the early streak (ES) stage (E6.75), prior to emVE dispersal, FN-1 was detected along the interface between epiblast and emVE, as a single belt separating these two tissue layers (Fig. 5a–c′). During early emVE dispersal (E7.0), when the wings of mesoderm were migrating anteriorly between the epiblast and emVE layers, one continuous belt of FN-1 was detected at the epiblast-mesoderm interface (Fig. 5d–f′). This BM was uninterrupted at the anterior extremities of the mesoderm and was contiguous with the BM lying anterior at the epiblast/emVE interface. FN-1 was also detected in patches near the mesoderm-endoderm interface, even though at this stage the separation between these two tissue layers was not evident (Fig. 5f, f′).

At the mid-emVE dispersal stage (E7.25), FN-1 localization at the epiblast-mesoderm interface remained unchanged, while at the mesoderm-endoderm interface it became uninterrupted (Fig. 5g–i′). At the late/complete emVE dispersal stage (E7.5) when mesoderm migration was complete, FN-1 localization was observed as two distinct, continuous belts: one between epiblast-mesoderm, and one between mesoderm-endoderm (Fig. 5j–l′). LAMININ-1 (LAMA-1), another BM component, exhibited a similar distribution to FN-1 during this developmental window (Supplementary Fig. 4a). Notably, the distribution of FN-1 and LAMA-1 in *Fgf8* or *Fgfr1* mutant embryos, as well as in epiblast-ablated *Eomes* embryos, invariably revealed a single BM between epiblast and emVE (Supplementary Fig. 4b). Together, these data reveal that mouse gastrulation involves a transition from one to two BMs. This must be coordinated with the migration of cells out of the primitive streak and generation of a new tissue layer.

During DE egression, we observed FN-1 and LAMA-1 localized at the prospective baso-lateral side of SOX17-positive DE cells, where they interfaced with other mesoderm cells, but not where they contacted emVE cells (Fig. 5m–p and Supplementary Fig. 4c–e). This suggested that egressing DE cells had acquired cell polarity and that *de novo* assembly of BM and/or remodeling of ECM was occurring baso-laterally in egressing DE cells.

Three-tissue layer configuration but only one basement membrane in *Sox17* mutants

As in wild-type, *Sox17* mutant embryos exhibited a continuous band of each of four ECM proteins (FN-1, LAMA-1, LAMB-1, and COLLAGEN IV (COLL-IV))at the epiblast-mesoderm interface (Fig. 5q–z′ and Supplementary Fig. 4f, g and Supplementary Video6). Even though three tissue layers were present in *Sox17* mutants, we failed to detect a BM at the mesoderm-endoderm interface, indicating that the formation of this BM requires SOX17.

To understand how the BM at the mesoderm-endoderm interface forms, we analyzed the expression of genes encoding ECM proteins by *in situ* hybridization. As gastrulation proceeded, *Fn1* was expressed by cells emanating from the primitive streak, the emVE cells overlying them, but not in emVE anterior to the mesoderm, nor in the epiblast (Supplementary Fig. 4h). *Lama1* exhibited a comparable expression pattern (data not shown). These data suggest that transcription of genes encoding ECM factors occurs concomitantly with cell migration from the primitive streak. Since previous studies have reported a role for SOX17 in ECM transcriptional regulation[20], we determined whether gene expression might be perturbed in *Sox17* mutants and found it to be unaffected (Supplementary Fig. 4i). This ruled out the direct transcriptional regulation of ECM proteins by SOX17 as a dominant mechanism causing the absence of a BM at the mesoderm-endoderm interface in *Sox17* embryos.

Egressing cells form E-CADHERIN rich cell-cell contacts with overlying emVE cells as an early step of epithelialization

The observation that non-egressed DE cells failed to epithelialize and remained within the mesodermal tissue layer in the absence of SOX17 raised the question of whether SOX17 might regulate the mesenchymal-to-epithelial transition (MET) of DE cells. We analyzed the localization of E-CADHERIN, which is commonly present at adherens junctions at the

interfaces of neighbouring epithelial cells[21]. In wild-type embryos prior to DE cell egression, E-CADHERIN localized at the interfaces of neighbouring VE cells as well as epiblast cells (Supplementary Fig. 5a–b6). At mid-emVE dispersal (E7.25), cells exiting the primitive streak and positioned within the mesoderm had downregulated E-cadherin (Fig. 6a–f). Egressing DE cells exhibited robust E-CADHERIN at their interface with emVE cells (Fig. 6a–f), indicating that they had acquired apico-basal polarity. Concomitant with DE cell egression, emVE cells had re-distributed their membrane-localized E-CADHERIN from their interface with neighbouring emVE cells to their interface with egressing DE cells. E-CADHERIN was also present in cells of the epiblast and emVE anterior to the leading edges of the mesoderm, as well as in ingressing cells within the primitive streak (Supplementary Fig. 5c–c6). Once gut endoderm morphogenesis was complete, E-CADHERIN localized at the interfaces of all cells within the gut endoderm epithelium regardless of their origin (Fig. 6g–l).

We quantified the levels of E-CADHERIN in egressing DE cells in wild-type and *Sox17* mutants. Measurement of fluorescent signal intensities in individual wild-type egressing cells revealed higher levels of E-CADHERIN on the reqion of their plasma membrane in proximity to the embryo's surface (Fig. 7a–d, m). In *Sox17* mutants, we failed to detect E-CADHERIN in cells within the mesodermal layer adjacent to the emVE (Fig. 7a′–d′, m′), suggesting that in the absence of SOX17, these cells failed to express E-CADHERIN[22]. Further, in *Sox17* mutants, emVE cells adjacent to the mesoderm maintained E-CADHERIN localization at their interfaces, with the epithelium generally appearing more organized than wild-type (Fig. 7c′, d′).

Egressing cells modulate distribution of cell polarity markers

To further investigate how cell polarity, another hallmark of epithelial cells, was modulated in DE and emVE cell populations, we analyzed the distribution of SCRIBBLE (SCRIB), which typically localizes to the baso-lateral domain of epithelial cells[23]. In wild-type embryos SCRIB exhibited an isotropic localization in inner cells of the mesodermal wings (Fig. 7e–h). By contrast, egressing cells displayed SCRIB polarization along their prospective apico-basal axis (Fig. 7g, h orange asterisks). Quantitation of signal confirmed that egressing cells had a higher degree of polarization compared to inner mesodermal cells (Fig. 7n). Interestingly, of 50 egressing cells analyzed, only 29 showed enrichment of SCRIB on their prospective basal side. The rest displayed enrichment of SCRIB on their prospective apical side. This suggested that, even though egressing cells distribute polarity markers in a biased way, the apical and basal domains can still change and are not irreversibly determined until cells are fully epithelialized. In *Sox17* mutants, SCRIB was localized uniformlyin inner cells of the mesoderm layer, and virtually all cells adjacent to the emVE exhibited enrichment of SCRIB at their interface with emVE cells (Fig. 7e′–h′, n). Hence, in *Sox17* mutants the emVE retains its epithelial integrity, and its baso-lateral distribution of SCRIB at the interface with the mesoderm. These observations underscore the inability of DE progenitors within the mesodermal layer to modulate the distribution of polarity markers in the absence of SOX17.

Definitive endoderm cells modulate deposition of BM-anchors during egression

Having noted that the absence of SOX17 did not affect ECM gene expression at a transcriptional level (Supplementary Fig. 4i), we investigated whether the absence of a BM at the mesoderm/gut endoderm interface in *Sox17* mutants resulted from a failure in BM assembly, possibly caused by modulation of cell polarity in either DE, emVE or both. From our previous analysis of gene expression profiles of the embryonic region of E7.5 embryos[7], we noted INTEGRIN-A5 (ITGA5), the receptor for FIBRONECTIN-1 (FN-1), as one of the predominant integrins expressed at this stage (Supplementary Fig. 6a). *In situ* analyses showed that in wild-type embryos at mid-emVE dispersal stages (E7.25), all cells in the mesodermal wings expressed ITGA5 (Fig. 7i–l). Egressing DE cells preferentially localized ITGA5 on their prospective basal side (Fig. 7k, l, o orange asterisks; Supplementary Fig. 6b–c′). By contrast, inner cells in the mesodermal wings displayed a uniform surface localization of ITGA5. The polarized distribution of ITGA5 in DE cells suggested it was being selectively trafficked and could account for ECM protein polymerizationon the prospective basal side to form a BM. We also found that in wild-type embryos, dispersing emVE cells exhibited polarized, albeit downregulated localization of ITGA5 in comparison to emVE cells in *Sox17* mutants (Fig. 7k, l pink asterisk and Fig. 7k′, l′), consistent with a transient reduction of aspects of polarity within wild-type emVE cells during DE cell egression. In *Sox17* mutants, cells in the mesodermal wings adjacent to the emVE did not localize ITGA5 on their prospective basal side (Fig. 7o, i′–l′). Instead, these cells always displayed enrichment on their prospective apical side, likely as a consequence of overlying emVE retaining its epithelial characteristics and therefore basal enrichment of ITGA5. Hence, even though SCRIB polarized to either apex of egressing cells, these cells must have acquired directionality in the apico-basal axis, considering that ITGA5 was consistently enriched on their prospective basal side.

DISCUSSION

In contrast to the prevailing view of strict lineage segregation in mammals, our data reveal that the gut endoderm comprises cells of both embryonic and extraembryonic origin. Here we demonstrate that cells that will form the DE originate within the primitive streak and migrate within, or aligned with, the mesoderm before intercalating into the VE on the embryo's surface. Our observations support the mechanism of endoderm morphogenesis proposed in the chick[24] where DE precursors ingress at the primitive streak, migrate within the mesodermal layer, insert into the extraembryonic endoderm layer, and transiently form a mosaic epithelium composed of embryonic and extra embryonic cells[25,26]. It has been suggested that chick extraembryonic endoderm cells persist and contribute to the developing liver[27]. Lineage tracing studies will be needed to determine whether emVE descendants contribute to adult endodermal tissues in mice.

Elucidating the gene regulatory network controlling DE formation has important implications for regenerative medicine. The evolutionarily-conserved transcription factors SOX17 and FOXA2 mark DE progenitors prior to their intercalation onto the embryo's surface. We observed that some posterior epiblast cells express FOXA2, but not SOX17, suggesting FOXA2 is the first marker of the DE lineage which is determined prior to

ingression through the primitive streak. However, our *in vivo* studies revealed that DE cell egression requires SOX17, but not FOXA2. Since *Foxa2* mutants express SOX17, this refutes a strict lineage specification dependence on FOXA2. The additional observation that FOXA2 is expressed in *Sox17* mutants suggests that SOX17 and FOXA2 likely act in parallel, but separate pathways.

Sox17 mutants exhibited limited emVE dispersal anteriorly, around the prospective foregut region (Fig. 2h). At later stages, *Sox17* mutants displayed defects in midgut and hindgut, leading to their developmental arrest and death at around E10.5[7]. Conversely, *Foxa2* mutants exhibit a primary defect in foregut and midline structures[28,29], with midgut and hindgut areas largely unaffected[30]. It is tempting to speculate that SOX17 controls gut endoderm morphogenesis in the prospective midgut and hindgut areas, and that foregut morphogenesis is orchestrated by FOXA2.

Our data identify the transition from a single BM positioned at the epiblast-visceral endoderm interface present before gastrulation, to two BMs positioned at the interfaces of epiblast-mesoderm and mesoderm-endoderm as gastrulation proceeds. Though *Sox17* mutants exhibit a trilaminar structure comprised of epiblast-mesoderm-VE, they possess only one BM, at the epiblast-mesoderm interface. Thus the BM at the mesoderm-endoderm interface is assembled at gastrulation, and its formation is associated with gut endoderm morphogenesis. SOX17 must have at least two critical, but not necessarily mutually-exclusive, roles: one regulating an endoderm identity, and another regulating cell polarity, and by extension epithelialization. Since the absence of SOX17 does not affect ECM gene expression (Supplementary Fig. 4i), the establishment of a BM at the mesoderm-endoderm interface likely results from post-transcriptionally regulated assembly, perhaps by baso-lateral clustering of proteins, for example integrins.

While much is known about how cells exit epithelia, limited attention has been paid to how cells enter them. For DE cells to egress into the emVE epithelium, DE and emVE cells must coordinately modulate their epithelial characteristics (Figure 8). DE cells adopt an epithelial identity including acquiring cell polarity, forming cell-cell junctions and exhibiting a biased deposition of BM. Concomitantly, emVE cells transiently relax their polarity, redistribute junctions, and can temporarily be relocated away from an underlying BM so as to accommodate the incoming DE cell flux. After cell egression is complete, this mixed population of cells (the gut endoderm) reinforce their epithelial qualities with BM forming *de novo* underneath them, there by facilitating their segregation from the mesoderm. It will be important to determine whether aspects of this cellular and molecular program control MET in the metastatic colonization of cancers of endoderm-derived tissues and organs.

METHODS

Mouse husbandry and strain genotyping

Mouse strains used in this study were: *Sox17*$^{cKO/cKO}$ and *Sox17*^{GFP}[31], *Fgf8*$^{+/-}$[32], *Fgfr1*$^{+/-}$[33], *Eomes*$^{cKO/cKO}$[34], *Foxa2*$^{+/-}$[35], *Sox2::Cre*$^{Tg/+}$[36], *Afp::GFP*$^{Tg/+}$[37, 38] and wild-type CD-1 (Charles River). The *Sox17*^{cKO} was used to generate the null *Sox17*^{KO} allele by crossing to the *Sox2::Cre* strain. PCR genotyping was performed as previously described.

Mouse husbandry and embryo experiments were performed in accordance with Memorial Sloan Kettering Cancer Center Institutional Animal Care and Use Committee-approved protocols. For all experiments, males and females were used indiscriminately.

Embryo recovery, manipulation and *ex utero* culture

Mice were maintained under a 12-hour light/dark cycle. Embryos were dissected in DMEM/F12 (Gibco) containing 5% fetal calf serum (Lonza) and staged according to Downs and Davies[39]. For live imaging, embryos were cultured in 50% Rat Serum;50% DMEM/F12[40].

Embryo electroporation

Electroporation of DNA constructs was performed as previously described[41]. *CAG::mRFP1 or CAG::myr-mCherry* constructs[42, 43] were electroporated into the primitive streak region of MS (E6.75) stage *Afp::GFP* embryos. A solution of DMEM/F12 (Gibco) containing ~3 μg/μl plasmid was micro-injected into the proamniotic cavity. Embryos were moved to pH7.5 Tyrode Ringer's solution and Tweezertrodes™ placed on either side of the embryo, with the anode positioned posteriorly. An ECM830 Square Wave Electroporator (BTX Harvard Apparatus) was used to deliver 5 pulses of 15–17V charge. After electroporation, embryos were washed in DMEM/F12 and processed for live imaging[44].

In situ hybridization and immuno-fluorescence

For in situ hybridization (ISH), embryos were fixed in 4% PFA in PBS overnight at 4°C, dehydrated in methanol and stored at −20°C. ISH was performed using antisense riboprobes as described previously[38]. Immuno-fluorescence was carried out as previously described[38]. Primary antibodies were used: COLL-IV (1:300, Millipore), FN-1 (1:300, Rockland), FOXA2 (1:1000, Abcam), LAMA-1 (1:300, Sigma), LAMB-1 (1:300, Abcam) and SOX17 (1:1000, R&D Systems) ITGA5 (1:300, Santa Cruz), E-CAD (1:300, Sigma), N-CAD (1:300, Santa Cruz), and SCRIB (1:200, Santa Cruz). Secondary Alexa-Fluor conjugated antibodies (Invitrogen) were used at a dilution of 1:1000. DNA was visualized using Hoechst-33342 (5 μg/mL, Molecular Probes). For cryosections, fixed embryos were taken through a sucrose gradient, embedded in O.C.T. (Tissue-Tek) and sectioned at 12 μm on a cryostat (CM3050S, Leica).

Image data acquisition, processing and quantitation

Wide field images were collected with Zeiss AxiocamMRc/m CCD cameras mounted on a Leica MZ165FC microscope. Confocal images were acquired using a Zeiss LSM510META or LSM700 as described previously[45, 46]. Fluorescence was excited with a 405-nm diode laser (Hoechst-33342), 488-nm Argon laser (GFP), 543-nm HeNe laser (AlexaFluor-543/555) and 633-nm HeNe laser (AlexaFluor-633/647). Images were acquired using Plan-Apo 20x/NA0.75 and Fluar 5x/NA0.25 objectives, with 0.2–2μm z-separation. For live imaging experiments, embryos were maintained in a temperature-controlled, humidified chamber with 5% CO_2 atmosphere as described previously[44]. Raw data were processed using ZEN or Imaris software (Zeiss and Bitplane respectively) and assembled in Photoshop CS6 (Adobe). Digital quantitation of immuno-fluorescent signal intensities was

performed using ZEN software (see Supplementary Fig. 7 and Supplementary Table 1). In all figures, representative images were selected from N>6 embryos. No statistical method was used to predetermine sample size, no experiments were randomized, and the investigators were not blinded to allocation during experiments and outcome assessment. No samples were excluded from the analysis.

Supplementary Material

Refer to Web version on PubMed Central for supplementary material.

Acknowledgments

We thank G. Kwon for implementing and optimizing the embryo electroporation technique and live imaging; M. Pulina for assistance with analysis of FGF signalling mutants; R. Turnbull for assistance with embryo cryosectioning; V. Seshan of the MSKCC Biostatistics Core Facility for advice on fluorescence intensity quantitations; J. Darnell, G. Martin, S. Morrison, C-a. Mao and J. Rossant for mouse lines; K. Anderson, M. Baylies and members of our laboratory for discussions and comments on the manuscript. This work was supported by the NIH (RO1-HD052115 and RO1-DK084391). MV was supported by a Frank J. Lappin Horsfall fellowship for part of this work. SN was supported by a Muscular Dystrophy Association Development Grant (186552).

References

1. Nowotschin S, Hadjantonakis AK. Cellular dynamics in the early mouse embryo: from axis formation to gastrulation. Curr Opin Genet Dev. 2010; 20:420–427. [PubMed: 20566281]
2. Arnold SJ, Robertson EJ. Making a commitment: cell lineage allocation and axis patterning in the early mouse embryo. Nat Rev Mol Cell Biol. 2009; 10:91–103. [PubMed: 19129791]
3. Rivera-Perez JA, Hadjantonakis AK. The Dynamics of Morphogenesis in the Early Mouse Embryo. Cold Spring Harbor perspectives in biology. 2014; a01586710.1101/cshperspect.a015867
4. Zorn AM, Wells JM. Vertebrate endoderm development and organ formation. Annu Rev Cell Dev Biol. 2009; 25:221–251. [PubMed: 19575677]
5. Viotti M, Nowotschin S, Hadjantonakis AK. Afp::mCherry, a red fluorescent transgenic reporter of the mouse visceral endoderm. Genesis. 2011; 49:124–133. [PubMed: 21442721]
6. Kwon GS, Viotti M, Hadjantonakis AK. The endoderm of the mouse embryo arises by dynamic widespread intercalation of embryonic and extraembryonic lineages. Dev Cell. 2008; 15:509–520. [PubMed: 18854136]
7. Viotti M, Niu L, Shi SH, Hadjantonakis AK. Role of the gut endoderm in relaying left-right patterning in mice. PLoS biology. 2012; 10:e1001276. [PubMed: 22412348]
8. Mesnard D, Guzman-Ayala M, Constam DB. Nodal specifies embryonic visceral endoderm and sustains pluripotent cells in the epiblast before over taxial patterning. Development. 2006; 133:2497–2505. [PubMed: 16728477]
9. Kwon GS, et al. Tg (Afp-GFP) expression marks primitive and definitive endoderm lineages during mouse development. Dev Dyn. 2006; 235:2549–2558. [PubMed: 16708394]
10. Yamaguchi TP, Harpal K, Henkemeyer M, Rossant J. fgfr-1 is required for embryonic growth and mesodermal patterning during mouse gastrulation. Genes Dev. 1994; 8:3032–3044. [PubMed: 8001822]
11. Ciruna B, Rossant J. FGF signaling regulates mesoderm cell fate specification and morphogenetic movement at the primitive streak. Dev Cell. 2001; 1:37–49. [PubMed: 11703922]
12. Sun X, Meyers EN, Lewandoski M, Martin GR. Targeted disruption of Fgf8 causes failure of cell migration in the gastrulating mouse embryo. Genes Dev. 1999; 13:1834–1846. [PubMed: 10421635]
13. Nowotschin S, et al. The T-box transcription factor Eomesodermin is essential for AVE induction in the mouse embryo. Genes Dev. 2013; 27:997–1002. [PubMed: 23651855]

14. Teo AK, et al. Pluripotency factors regulate definitive endoderm specification through eomesodermin. Genes Dev. 2011; 25:238–250. [PubMed: 21245162]
15. Arnold SJ, Hofmann UK, Bikoff EK, Robertson EJ. Pivotal roles for eomesodermin during axis formation, epithelium-to-mesenchyme transition and endoderm specification in the mouse. Development (Cambridge, England). 2008; 135:501–511.
16. Kanai-Azuma M, et al. Depletion of definitive gut endoderm in Sox17-null mutant mice. Development (Cambridge, England). 2002; 129:2367–2379.
17. Seguin CA, Draper JS, Nagy A, Rossant J. Establishment of endoderm progenitors by SOX transcription factor expression in human embryonic stem cells. Cell Stem Cell. 2008; 3:182–195. [PubMed: 18682240]
18. Stainier DY. A glimpse into the molecular entrails of endoderm formation. Genes & development. 2002; 16:893–907. [PubMed: 11959838]
19. Kim I, Saunders TL, Morrison SJ. Sox17 dependence distinguishes the transcriptional regulation of fetal from adult hematopoietic stem cells. Cell. 2007; 130:470–483. [PubMed: 17655922]
20. Niakan KK, et al. Sox17 promotes differentiation in mouse embryonic stem cells by directly regulating extraembryonic gene expression and indirectly antagonizing self-renewal. Genes Dev. 2010; 24:312–326. [PubMed: 20123909]
21. Baum B, Georgiou M. Dynamics of adherens junctions in epithelial establishment, maintenance, and remodeling. The Journal of cell biology. 2011; 192:907–917. [PubMed: 21422226]
22. Roh MH, Margolis B. Composition and function of PDZ protein complexes during cell polarization. American journal of physiology. Renal physiology. 2003; 285:F377–387. [PubMed: 12890661]
23. Humbert PO, Dow LE, Russell SM. The Scribble and Par complexes in polarity and migration: friends or foes? Trends in cell biology. 2006; 16:622–630. [PubMed: 17067797]
24. Vakaet L. Some new data concerning the formation of the definitive endoblast in the chick embryo. Journal of embryology and experimental morphology. 1962; 10:38–57. [PubMed: 13924249]
25. Azar Y, Eyal-Giladi H. The retention of primary hypoblastic cells underneath the developing primitive streak allows for their prolonged inductive influence. Journal of embryology and experimental morphology. 1983; 77:143–151. [PubMed: 6655430]
26. Kimura W, Yasugi S, Stern CD, Fukuda K. Fate and plasticity of the endoderm in the early chick embryo. Developmental biology. 2006; 289:283–295. [PubMed: 16337933]
27. Bertocchini F, Stern CD. A differential screen for genes expressed in the extraembryonic endodermal layer of pre-primitive streak stage chick embryos reveals expression of Apolipoprotein A1 in hypoblast, endoblast and endoderm. Gene expression patterns : GEP. 2008; 8:477–480. [PubMed: 18672094]
28. Ang SL, Rossant J. HNF-3 beta is essential for node and notochord formation in mouse development. Cell. 1994; 78:561–574. [PubMed: 8069909]
29. Weinstein DC, et al. The winged-helix transcription factor HNF-3 beta is required for notochord development in the mouse embryo. Cell. 1994; 78:575–588. [PubMed: 8069910]
30. McKnight KD, Hou J, Hoodless PA. Foxh1 and Foxa2 are not required for formation of the midgut and hindgut definitive endoderm. Developmental biology. 2010; 337:471–481. [PubMed: 19896480]
31. Kim I, Saunders TL, Morrison SJ. Sox17 dependence distinguishes the transcriptional regulation of fetal from adult hematopoietic stem cells. Cell. 2007; 130:470–483. [PubMed: 17655922]
32. Meyers EN, Lewandoski M, Martin GR. An Fgf8 mutant allelic series generated by Cre- and Flp-mediated recombination. Nat Genet. 1998; 18:136–141. [PubMed: 9462741]
33. Yamaguchi TP, Harpal K, Henkemeyer M, Rossant J. fgfr-1 is required for embryonic growth and mesodermal patterning during mouse gastrulation. Genes Dev. 1994; 8:3032–3044. [PubMed: 8001822]
34. Mao CA, et al. Eomesodermin, a target gene of Pou4f2, is required for retinal ganglion cell and optic nerve development in the mouse. Development. 2008; 135:271–280. [PubMed: 18077589]
35. Weinstein DC, et al. The winged-helix transcription factor HNF-3 beta is required for notochord development in the mouse embryo. Cell. 1994; 78:575–588. [PubMed: 8069910]

36. Hayashi S, Lewis P, Pevny L, McMahon AP. Efficient gene modulation in mouse epiblast using a Sox2Cre transgenic mouse strain. Mechanisms of development. 2002; 119 (Suppl 1):S97–S101. [PubMed: 14516668]

37. Kwon GS, et al. Tg (Afp-GFP) expression marks primitive and definitive endoderm lineages during mouse development. Dev Dyn. 2006; 235:2549–2558. [PubMed: 16708394]

38. Kwon GS, Viotti M, Hadjantonakis AK. The endoderm of the mouse embryo arises by dynamic widespread intercalation of embryonic and extraembryonic lineages. Dev Cell. 2008; 15:509–520. [PubMed: 18854136]

39. Downs KM, Davies T. Staging of gastrulating mouse embryos by morphological landmarks in the dissecting microscope. Development. 1993; 118:1255–1266. [PubMed: 8269852]

40. Jones, EAV.; Hadjantonakis, AK.; Dickinson, ME. Imaging Mouse Embryonic Development. In: Yuste, R.; Konnerth, A., editors. Imaging in NEuroscience and Development. Cold Spring Harbor Laboratory Press; Cold Spring Harbor, NY: 2005.

41. Khoo PL, Franklin VJ, Tam PPL. Fate-Mapping Technique: Targeted Whole-Embryo Electroporation of DNA Constructs into the Germ Layers of Mouse Embryos 7–7.5 Days Post-coitum. Cold Spring Harb Protoc. 200710.1101/pbd.prot4893

42. Long JZ, Lackan CS, Hadjantonakis AK. Genetic and spectrally distinct in vivo imaging: embryonic stem cells and mice with widespread expression of a monomeric red fluorescent protein. BMC Biotechnol. 2005; 5:20. [PubMed: 15996270]

43. Nowotschin S, Eakin GS, Hadjantonakis AK. Dual transgene strategy for live visualization of chromatin and plasma membrane dynamics in murine embryonic stem cells and embryonic tissues. Genesis. 2009; 47:330–336. [PubMed: 19358158]

44. Nowotschin S, Ferrer-Vaquer A, Hadjantonakis AK. Imaging mouse development with confocal time-lapse microscopy. Methods in enzymology. 2010; 476:351–377. [PubMed: 20691876]

45. Viotti M, Nowotschin S, Hadjantonakis AK. Afp::mCherry, a red fluorescent transgenic reporter of the mouse visceral endoderm. Genesis. 2011; 49:124–133. [PubMed: 21442721]

46. Viotti M, Niu L, Shi SH, Hadjantonakis AK. Role of the gut endoderm in relaying left-right patterning in mice. PLoS biology. 2012; 10:e1001276. [PubMed: 22412348]

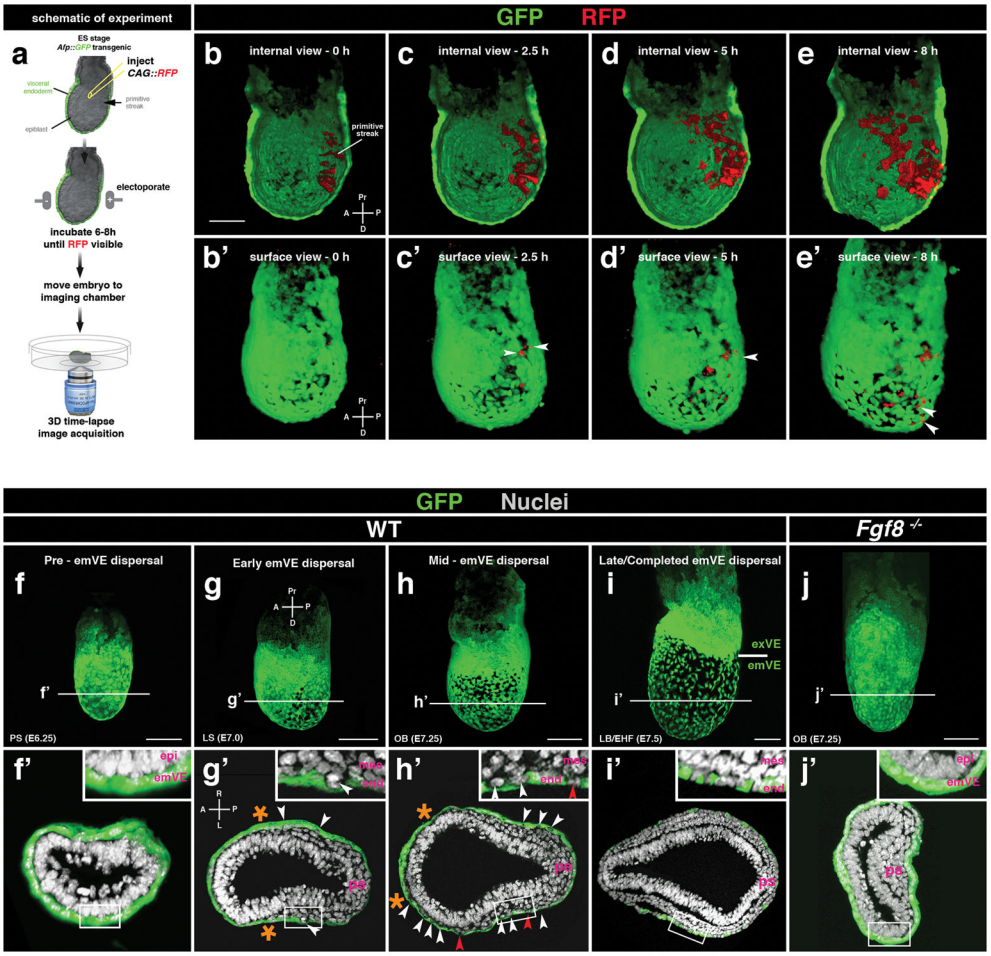

Figure 1. DE cells originate in the posterior epiblast and migrate with the wings of mesoderm before egressing into the emVE epithelium

(a) Schematic depicting the electroporation and time-lapse imaging procedure.

(b–e) Interior rendered views from a time-lapse.

(b′–e′) Surface rendered views from a time-lapse (b–e).

(f–i) *Afp::GFP* VE-reporter embryos showing progression of emVE dispersal from pre-dispersal (PS stage, E6.25) to late/completed dispersal (LB/EHF stage, E7.5) stage.

(f′–i′) Transverse sections through *Afp::GFP* embryos in (f–i).

(j and j′) Whole mount view and transverse section of *Fgf8* mutant, transgenic for the *Afp::GFP* VE-reporter, showing accumulation of cells in the area of the primitive streak and no emVE dispersal.

ps, primitive streak; emVE, embryonic visceral endoderm; epi, epiblast; exVE, extraembryonic visceral endoderm; mes, mesoderm; A, anterior; D, distal; L, left; P, posterior; Pr, proximal; R, right; PS, pre-streak; LS, late streak; OB, no bud; LB, late bud; EHF, early head-fold. Scale bars = 100 μm.

See also Supplementary Fig. 1 and Supplementary Videos 1–5.

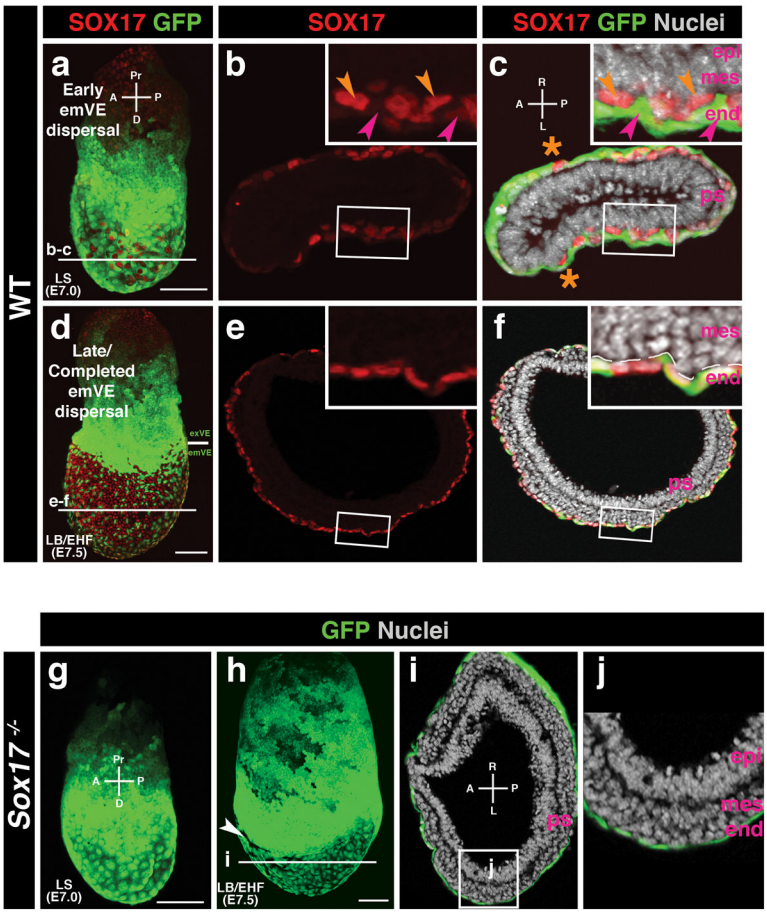

Figure 2. SOX17 marks DE cells prior to, during, and after egression and is required for egression event

(a) Whole mount image of immuno-fluorescence for SOX17 in an *Afp::GFP* VE-reporter embryo at the early emVE dispersal stage.

(b and c) Sections through embryo in (a) indicate two different expression levels of SOX17 during early emVE dispersal. EmVE cells display low levels of SOX17 (pink arrowheads), and DE cells in the process of egressing display high levels of SOX17 (orange arrowheads). Orange asterisks mark the leading edge of the mesoderm.

(d) Whole mount image of immuno-fluorescence for SOX17 in an *Afp::GFP* VE-reporter embryo at the late/completed emVE dispersal stage.

(e and f) Sections through embryo in (d) indicate equal levels of SOX17 expression in all cells of the gut endoderm layer, regardless if emVE-derived (GFP-positive) or of the DE lineage (GFP-negative).

(g) *Sox17* mutant *Afp::GFP* VE-reporter embryo at the LS stage displays a solid layer of GFP-positive cells on its distal surface.

(h) *Sox17* mutant *Afp::GFP* VE-reporter embryo at the LB/EHF stage showing a uniform layer of GFP-positive cells on its distal surface, suggesting continuous failure of DE-cell egression. Limited egression of DE cells into the emVE has occurred anteriorly in the area around the prospective foregut invagination (white arrowhead).

(i and j) Low and high magnifications of sections through *Sox17* mutant embryo in (h) show wings of mesoderm that have completed anterior migration and a solid GFP-positive layer on the surface of the embryo, representing the undispersed emVE epithelium.
ps, primitive streak; end, endoderm; epi, epiblast; mes, mesoderm; A, anterior; D, distal; L, left; P, posterior; Pr, proximal; R, right; LS, late streak; LB, late bud; EHF, early head-fold. Scale bars = 100 μm.
See also Supplementary Fig. 2.

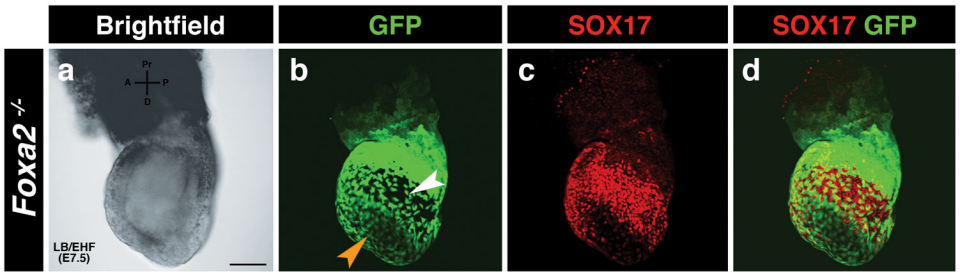

Figure 3. FOXA2 is not required for DE cell egression or SOX17 expression

(a–d) Whole mount images of *Foxa2* mutant expressing the *Afp::GFP* VE-reporter at the LB/EHF (E7.5) stage, with immuno-fluorescence for SOX17. Note that the midline has failed to undergo correct formation (orange arrowhead), but the emVE has undergone dispersal (white arrowhead).

A, anterior; D, distal; P, posterior; Pr, proximal; LB, late bud; EHF, early head-fold. Scale bar = 100 μm.

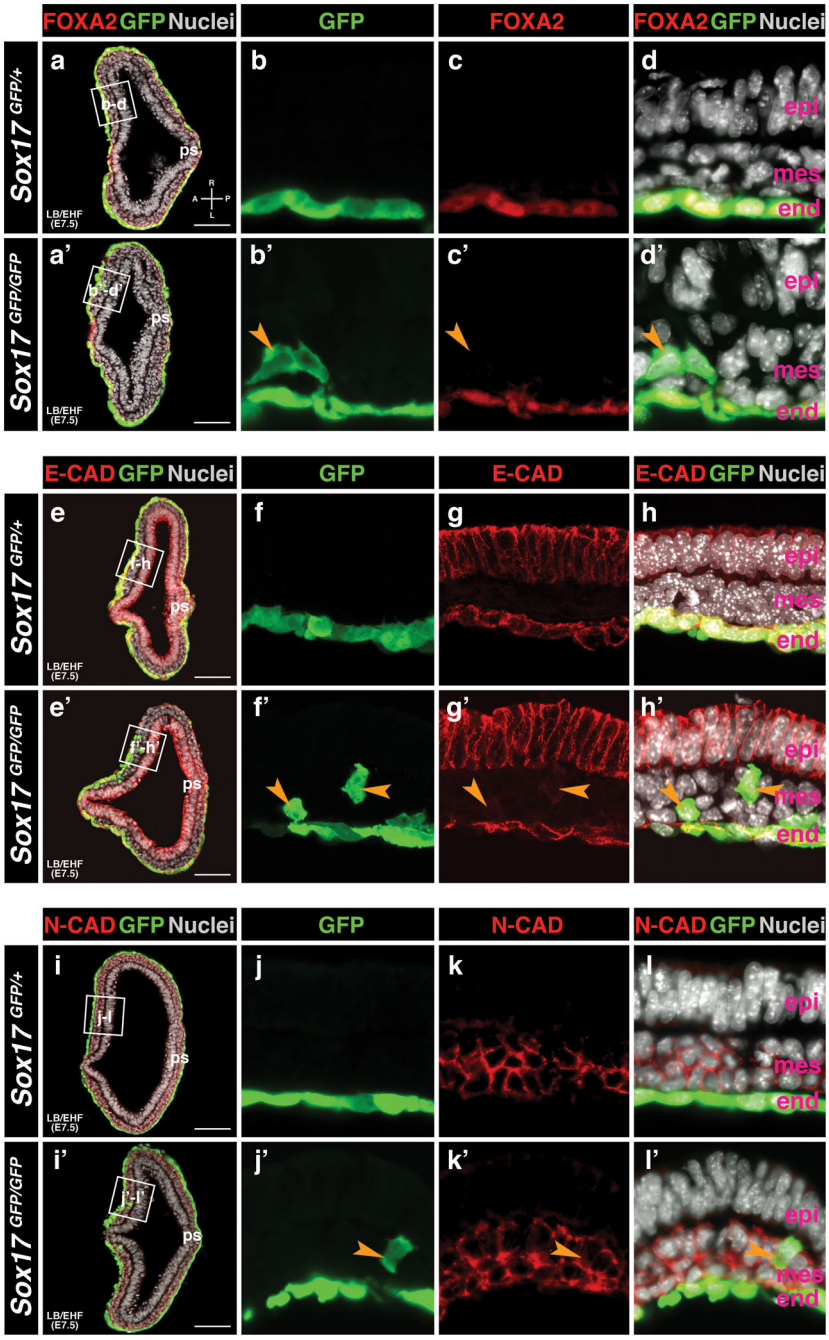

Figure 4. Cells failing to egress remain within the mesodermal wings

(a–d) Low and high magnifications of sections through a LB/EHF stage (E7.5) *Sox17*$^{GFP/+}$ embryo with immuno-fluorescence for the endoderm marker FOXA2, indicating a single layer of GFP-positive cells on the surface of the embryo (all cells of the gut endoderm), uniformly expressing FOXA2.

(a′–d′) A *Sox17*$^{GFP/GFP}$ embryo additionally displays some GFP-positive cells embedded within the mesodermal layer and do not express FOXA2(orange arrowheads).

(e–h) Low and high magnification views of sections through a *Sox17*$^{GFP/+}$ embryo depicting immuno-fluorescence for the epithelial marker E-CADHERIN (E-CAD). Fluorescent signal is present between cells in the epiblast layer and in the gut endoderm, which is GFP-positive.

(e′–h′) A *Sox17*$^{GFP/GFP}$ embryo additionally displays some GFP-positive cells within the wings of mesoderm. These 'non-egressed' cells show low levels of cytoplasmic E-CAD (orange arrowheads).

(i–l) Low and high magnifications of sections through a *Sox17*$^{GFP/+}$ embryo depicting immuno-fluorescence for the mesenchymal marker N-CADHERIN (N-CAD). N-CAD stain is present between cells of the wings of mesoderm, and absent from cells of the epiblast or the gut endoderm, which is GFP-positive.

(i′–l′) A *Sox17*$^{GFP/GFP}$ embryo additionally displays some GFP-positive cells within the wings of mesoderm. These 'non-egressed' cells show N-CAD at their interface with neighbouring mesodermal cells (orange arrowheads).

ps, primitive streak; emVE, embryonic visceral endoderm; end, endoderm; epi, epiblast; exVE, extraembryonic visceral endoderm; mes, mesoderm; A, anterior; D, distal; L, left; P, posterior; Pr, proximal; R, right; LB, late bud; EHF, early head-fold. Scale bars = 100 μm. See also Supplementary Fig. 3.

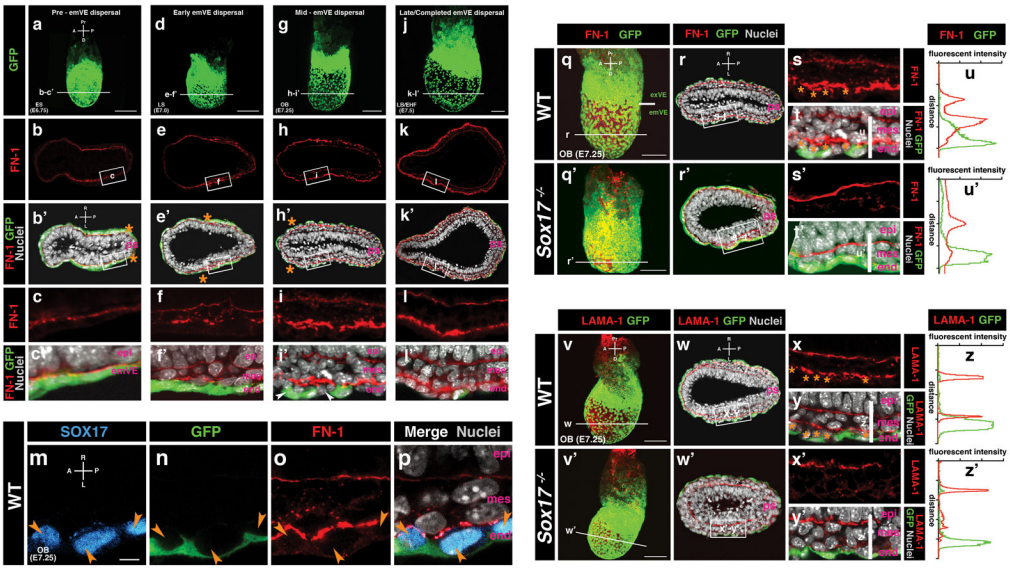

Figure 5. Formation of basement membrane at mesoderm-endoderm interface does not occur in *Sox17* mutants

(a–l′) Immuno-fluorescence for the BM protein FN-1 in *Afp::GFP* VE-reporter embryos.

(a–c′) At the ES stage (E6.75), shortly after the wings of mesoderm have begun their anterior migration (leading tips indicated by orange asterisks), a single continuous signal for FN-1 is present between epiblast and the GFP-positive emVE.

(d–f′) During early emVE dispersal, one BM is visible anterior to the leading tips of the wings of mesoderm (orange asterisks), and two BMs in regions where the wings of mesoderm are present. The BM between mesoderm and endoderm is heavily fenestrated.

(g–i′) FN-1 at mid-emVE dispersal identifies two BMs where the wings of mesoderm are present.

(j–l′) FN-1 at the late/completed emVE dispersal stage identifies two solid BMs separating germ layers.

(m–p) Double stains in *Afp::GFP* VE-reporter embryo shows egressing DE cells with high levels of SOX17 in the process of inserting between emVE cells displaying FN-1 basally. EmVE cells never display FN-1 at their interface with egressing DE cells.

(q–t) Stained *Afp::GFP* VE-reporter wild-type embryo showing egressing DE cells (orange asterisks) always display FN-1 basally.

(q′–t′) In the *Sox17* mutant, the interface between mesoderm and emVE only displays faint punctate FN-1 fluorescent signal.

(u and u′) Digital quantitation of FN-1 fluorescent signal indicating two peaks in the wild-type and only one peak in the *Sox17* mutant.

(v–y) Stained *Afp::GFP* VE-reporter wild-type embryo showing egressing DE cells (orange asterisks) always display LAMA-1 basally.

(v′–y′) In *Sox17* mutants, the interface between mesoderm and emVE displays punctate LAMA-1 fluorescent signal, similarly to the puncta interspersed between cells of the wings of mesoderm of the wild-type.

(z and z′) Digital quantitation of fluorescent signal indicating two peaks for LAMA-1 in the wild-type, and only one in *Sox17* mutant.

ps, primitive streak; emVE, embryonic visceral endoderm; end, endoderm; epi, epiblast; mes, mesoderm; A, anterior; D, distal; L, left; P, posterior; Pr, proximal; R, right; PS, pre-streak; LS, late streak; OB, no bud; LB, late bud; EHF, early head-fold. Scale bars = 20 μm in panel m, 100 μm in all other panels.

See also Supplementary Fig. 4 and Supplementary Video 6.

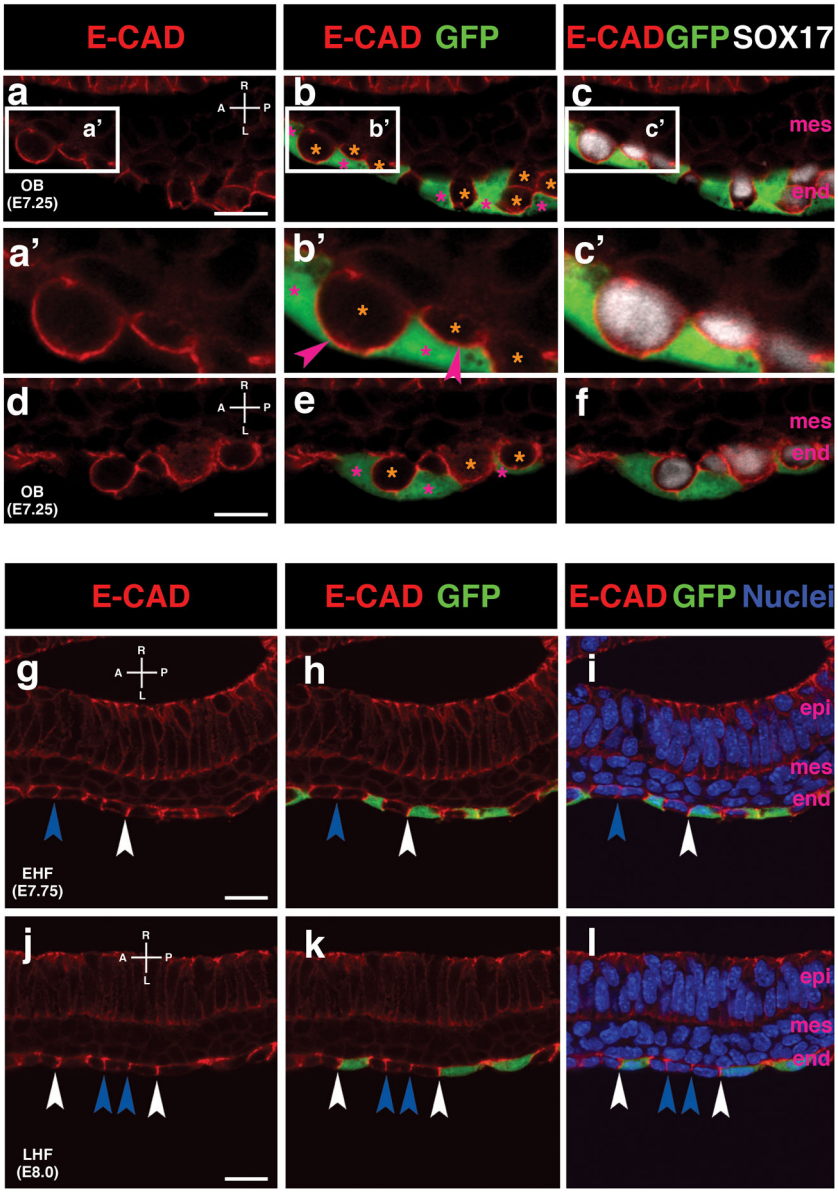

Figure 6. E-CADHERIN distribution dynamics in DE and emVE cells

(a–f) High magnifications of sectioned OB (E7.25) *Afp::GFP* VE-reporter wild-type embryos stained for E-CAD and SOX17. Strong white signal indicates egressing DE-cells (orange asterisks) in the process of inserting between GFP-positive emVE cells (pink asterisks). Note the polarization of E-CAD signal in egressing cells, with strong localization (pink arrowheads) on their cell membrane interfacing with emVE cells.

(g–l) E-CAD stain in EHF (E7.75) and LHF (E8.0) stage *Afp::GFP* VE-reporter wild-type embryos. Note the strong localization of E-CAD in the gut endoderm between fully egressed DE cells (blue arrowheads) as well as at the interface between DE and GFP-positive emVE-derived cells (white arrowheads).

end, endoderm; epi, epiblast; mes, mesoderm; A, anterior; L, left; P, posterior; R, right; OB, no bud; EHF, early head-fold; LHF, late head-fold. Scale bars = 20μm.

See also Supplementary Fig. 5.

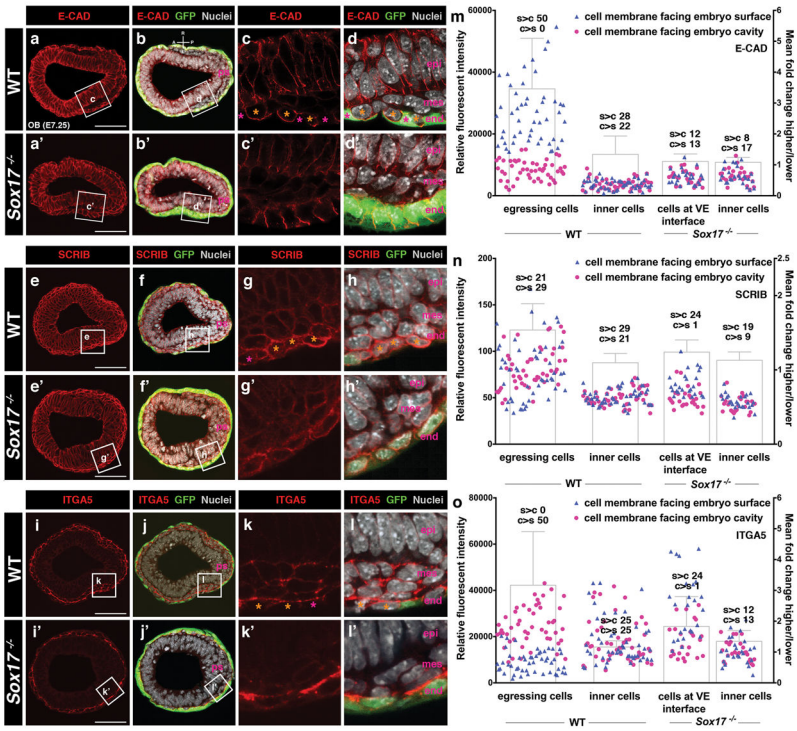

Figure 7. DE cells in *Sox17* mutants fail to epithelialize

(m–o) Digital quantitation of fluorescent intensities. In six or more wild-type embryos, we measured 50 egressing cells and 50 inner cells (deeper in the mesoderm layer). In >6 *Sox17* mutants, we measured 25 cells at the interface with the VE and 25 inner cells. Dot plot of two measurements made for each cell; one for the cell's apex facing the embryo surface (blue triangles) and the other for the apex facing the embryo cavity (purple dots) (see Supplementary Fig. 7). Numbers above the graph indicate the instances in which the measurement on the side of the embryo ***s***urface was higher or lower than the measurement on the side of the embryo ***c***avity. Histogram indicates the mean ratio between higher and lower value for each cell type (n=50 for wild-type cells, n=25 in mutant cells). Error bars represent standard deviation.

ps, primitive streak; end, endoderm; epi, epiblast; mes, mesoderm; A, anterior; L, left; P, posterior; R, right; OB, no bud; s, side of embryo surface; c, side of embryo cavity. Scale bars = 100 μm.

See also Supplementary Figs. 6 and 7.

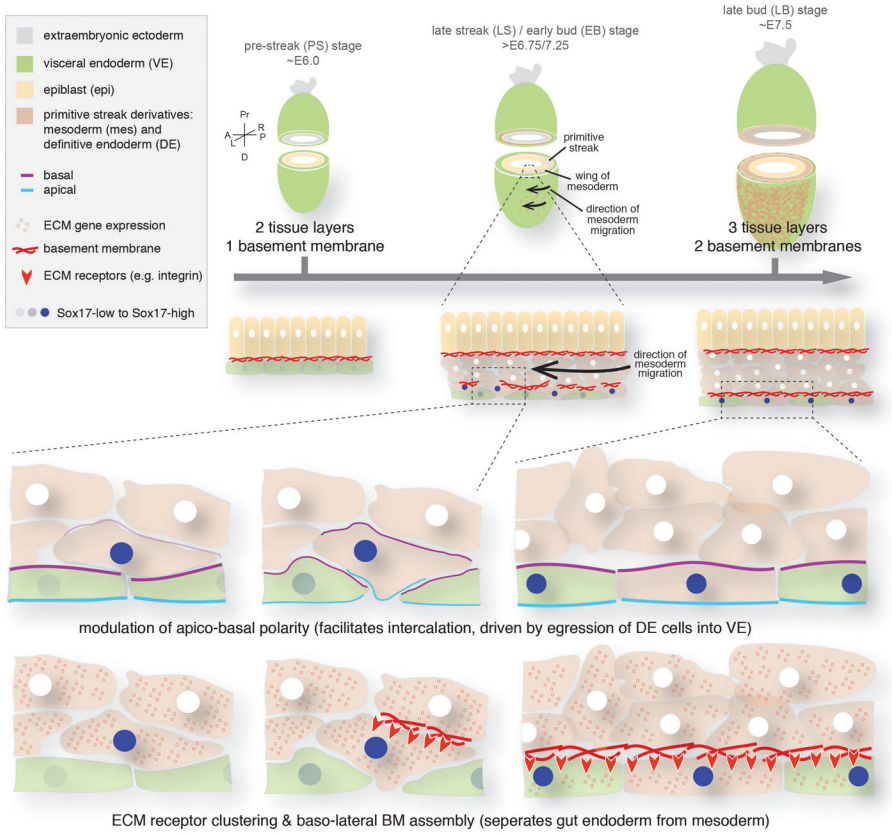

Figure 8. Working model of cell behaviors during gut endoderm morphogenesis and germ layer segregation in mice

The gut endoderm forms by widespread intercalation between embryonic and extra-embryonic endoderm, which occurs concomitantly with the assembly of a BM at its interface with the mesoderm. Gastrulation transforms a two-layered to a three-tissue layered tissue configuration. Epiblast cells ingress and undergo EMT at the primitive streak. They emerge as mesoderm or gut endoderm. SOX17 orchestrates a mesenchymal-to-epithelial transition (MET) of DE cells at the interface with the VE, in which DE cells become polarized, enrich ECM receptors, and assemble BM components basally. The overlying VE layer transiently moderates its epithelial characteristics, facilitating DE cell egression. The emergent gut endoderm (composed of VE and DE cells) subsequently reinforces the underlying BM, segregating mesoderm from gut endoderm tissue layers.